Available online at www.sciencedirect.com
ScienceDirect
International Journal of Thermal Sciences 46 (2007) 1285–1296
International Journal of Thermal Sciences
www.elsevier.com/locate/ijts

Influence of geometrical factors and pressing mould wear on thermal-hydraulic characteristics for steel offset strip fins at low Reynolds number

Lihua Guo [a,*], Feng Qin [a], Jiangping Chen [a], Zhijiu Chen [a], Yimin Zhou [b]

[a] *Institute of Refrigeration and Cryogenics Engineering, Shanghai Jiaotong University, 1954 Huashan Road, Shanghai 200030, PR China*
[b] *Zhejiang Yinlun Machinery Co. Ltd., Zhejiang Province 317200, PR China*

Received 18 March 2006; received in revised form 22 December 2006; accepted 22 December 2006

Available online 14 February 2007

Abstract

Aiming at achieving a more comprehensive understanding of influence factors on thermal-hydraulic characteristics for high-pressure-direction type steel offset strip fins, this paper constructed a single fin core assembly test rig with lubricant oil as work media at low Reynolds number. Six fin schemes were experimentally investigated only varying in fin height and fin wavelength due to mould restrictions. Twenty fin schemes changing in fin width, fin angle, fin thickness and staggered fin wavelength were simulated for supplement, and the geometrical influences in fin performance were put forward. Both Taguchi method and uniform design were introduced to study the contribution of each geometrical factor to fin global thermal-hydraulic performance, verifying that fin wavelength and fin height have the most significant contributions. Based on signal to noise ratio distributions, fin geometries were optimized for 16% elevation of global performance at Reynolds number of 430, then the 'cost-based fin performance' was put forward and compared quantitatively, proving that above optimum fin scheme is also economical. Finally, mould wear influence in fin performance was tested in different wear periods of a vacuum heat-treated Cr12MoV mould pair, then three stages of initial wear, stable wear, and overdrive wear were defined based on pressing times. The influences were analyzed and regulations were deduced relating to mould pressing times and oil Reynolds number. The suggested lifetime for this type of mould pair is 1050 thousand pressing times. The paper intends for fin performance evaluation, optimization, and pressing mould improvement.

Keywords: Offset strip fin; Heat exchanger; Colburn factor; Friction factor; Optimization; Mould wear

1. Introduction

With the enhancement of heat exchange capacity, more compact heat exchangers with fins of higher thermal performance are needed in aircrafts, automobiles and HVACs. In engine cooling systems, offset strip fins are generally adopted in plate-fin oil coolers to cope with the increasing thermal loads [1]. The substantial heat transfer enhancement is obtained as the combined results that the staggered fins increase heat transfer surfaces, interrupt flow and temperature boundary layers along flow orientation, as well as lead to entrance effects and vortexes [2]. However, this heat transfer enhancement is at the expense of increasing pressure loss. A balance between thermal and hydraulic characteristics should be sought for heat exchanger optimization.

The most comprehensive study on offset strip fins was conducted by Muzychka [3]. His research divided offset strip fins into two categories according to fluid flow orientations, one is the High Pressure Direction (HPD), where the fluid impinges on fin surfaces; another is the Low Pressure Direction (LPD), where the fluid flows parallel to fin surfaces, as shown in Fig. 1. Usually the HPD type fins exhibit higher heat transfer characteristic and friction loss than those of the LPD type fins, of which the reason is that the staggered surfaces of the HPD type fins interrupt flow and temperature boundary layers more acutely.

* Corresponding author. Tel.: +86 21 6293 3242; fax: +86 21 6293 2601.
E-mail address: guolihua79@sjtu.edu.cn (L. Guo).

1290-0729/$ – see front matter
doi:10.1016/j.ijthermalsci.2006.12.009

Nomenclature

A	area	m^2
b	fin width	m
c_{oil}	oil specific heat capacity	$J\,kg^{-1}\,K^{-1}$
d_h	hydraulic diameter	m
h	fin height	m
h_{oil}	heat transfer coefficient	$W\,m^{-2}\,K^{-1}$
L	fin core flow length	m
l	fin effective length	m
M	mass	kg
m	degree of freedom	
m_{oil}	oil mass flow rate	$kg\,s^{-1}$
n	mould pressing times	
P	unit price	
p	pressure	Pa
Δp	pressure difference	Pa
S_m	mean variance of measure data	
SN	signal to noise ratio	
$\overline{SN}$	arithmetical mean signal to noise ratio	
s	fin wavelength	m
s_0	staggered fin wavelength	m
T	temperature	K
ΔT_m	log mean temperature difference	K
t	thickness	m
u	oil flow velocity	$m\,s^{-1}$
V_e	error sum of squares	
V_{free}	free flow volume	m^3
Z	number of effective replications	
x, y, z	spatial coordinates	

Greeks symbols

α	fin angle	deg
β	mass ratio of fin to two base plates	
η_o	heat transfer surface efficiency	
λ	heat conductivity	$W\,m^{-1}\,K^{-1}$
μ	dynamic viscosity	$kg\,m^{-1}\,s^{-1}$
ρ	density	$kg\,m^{-3}$

Subscripts

ba	bare channel without fin
cu	cooper plate
f	fin
in	inlet
m	mean
max	maximum
min	minimum
oil	oil side
out	outlet
p	plate
w	wall
wet	wetted surface

Dimensionless

C	cost ratio of whole plate-fin to two base plates
CER	cost-effect ratio
CR	contribution ratio
f	friction factor
j	Colburn factor
JF	thermal-hydraulic performance factor
Nu_{dh}	Nusselt number based on hydraulic diameter
Pr	Prandtl number
Re_{dh}	Reynolds number based on hydraulic diameter
Θ	dimensionless temperature

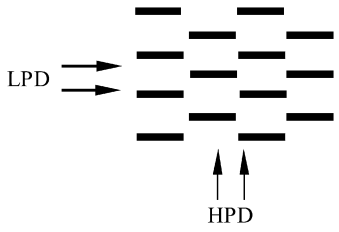

Fig. 1. Flow orientation definition for offset strip fins.

Lots of efforts have been devoted to heat transfer and friction characteristics of LPD type offset strip fins. Early experimental investigations on offset fin geometries were carried out by Kays and London [4–6], and their researches were summarized including the test results for twenty-one offset fin arrays in 1980's [7]. Hachemi [8] etc., extended these experimental researches to similar geometries. Additionally, Wieting [9] built the empirical correlations of Colburn factor j and friction factor f based on existing experimental data. Joshi and Webb [10] performed pressure drop tests on eight scale-up offset fin geometries and set up the analytical models for offset strip fins in laminar and turbulent flow. A thorough review of experimental research on LPD type offset fin geometries was reported by Manglik and Bergles [11], in which they complied and analyzed the heat transfer and friction factor for eighteen offset strip surfaces and also developed correlations to describe the asymptotic behavior of the data in the deep laminar and fully turbulent regions. However, the validity of their correlations for liquids is open to doubt. In addition, Muzychka et al. also set up the analytical models on LPD type fins [3,12] applied to laminar and transition flow regions. Despite above opening researches on LPD type fins, it is the well-known fact that since most of the enhanced heat transfer surfaces employed by the automotive industry are considered proprietary technology, details of the heat transfer and fluid friction characteristics are hardly published. The same thing happens to the HPD type offset strip fins. The only available study on HPD type fins is reported by Muzychka [3,13], in which the experimental data were gotten through the measurement of offset strip fins made of aluminum and brass. However, as a result of the manufacturing difference between the 'soft' materials of aluminum or brass and the 'hard' material of steel, during the punch process the steel fin surfaces are prone to produce more burrs and roughness than those of aluminum and brass, hence it is impractical to get the general thermal and

hydraulic models applied to offset strip fins made of different materials. The same cognition was mentioned by Manglik [11] and Sen [14] that manufacturing irregularities such as burred edges, bonding imperfections and separating plate roughness influence the flow and heat transfer characteristics in actual heat exchanger cores.

Comparing to all aforementioned literatures using air coolant except Muzychka's, very little experimental work has been published using liquid coolants on offset strip fin heat exchangers. Although Kays and London's literature [10] suggested that the results for air media are applied to those of liquid fluid, plenty of investigations denoted that Prandtl number effects of test media on thermal and hydraulic performance for enhanced surfaces are not negligible, especially for thermal characteristics [11,15,16]. In Sen's [15] investigation, the models for air overpredict the Colburn factor for liquid coolants up to about 100%, which is unacceptable in typical thermal design. Consequently it is limited to apply the correlations for air media to the higher Prandtl number liquid media. Since the offset strip fins are widely used in engine oil coolers, it is demanded to carry out the study taken lubricant oil as coolant for practical conditions.

In view of above references, experiment is a major method to study fin performances. However, continuous varying in all geometrical parameters for a wide range is costly and unfeasible, thus simulation is necessary to parametrical studies. Patankar [17] early simulated planar heat exchanger models regardless of fin height. Yang [18] and Costa [19] also investigated certain two-dimensional fin schemes. In recent years, Taguchi method has been adopted in construction design for heat exchangers to efficiently seek the combination of optimized design parameters [20–22], and in Refs. [20,21], the experimental investigations on heat exchangers validated the reliability of Taguchi Method. The researches denoted that in addition to keeping the experimental cost at the minimum level, one of the advantages of Taguchi method over the conventional experimental design methods is that it minimizes the variability around the target when bringing the performance value to the target value. Another advantage is that the optimum working conditions determined from the laboratory work can also be reproduced in the real production environment. As the purpose of this study is not to validate this method, it will not be explained here, which has been referred in the literatures by Kackar [23], Taguchi [24], and Phadke [25].

All above mentioned studies provide the motivation to investigate the HPD type steel fins using lubricant oil as coolant. Concerning the low velocity of coolant and the small hydraulic diameter for offset strip geometries in practice, the present research focuses on low Reynolds number less than 500. Aiming at getting rid of inlet flow maldistributions by multi-channel heat exchangers [26], a single fin core assembly test rig was constructed. In order to avoid mould wear effects, the tested fins were manufactured by the same mould simultaneously when mould wear was stable, thus only fin height and fin wavelength were studied experimentally. For a supplement of experiments, twenty schemes varying in all fin geometrical factors were numerically studied three-dimensionally including six geometrical parameters. Combining Taguchi method with uniform design technique, the importance of each fin geometrical factor was investigated, and geometrical optimizations were carried out for achieving prime fin global performance. Considering raw material consumption, the 'cost-effect ratio' was proposed and compared. Finally, mould wear influence was tested on performance of fins pressed by the same mould pair during different pressing times, and influence regulations were put forward. This research intends for a more comprehensive and accurate understanding of influence factors on HPD type steel offset strip fins, which would be helpful to fin performance evaluation, optimization, and pressing mould improvement.

2. Fin schemes

As shown in Fig. 2, lubricant oil and water commonly flow counter-currently in engine oil coolers. Offset strip fins are installed in oil side in order to enhance oil side heat transfer. The material of the tested HPD type fins is made of SPCC, a kind of low carbon steel. They were pressed by cold stamping mould, and cut into 245 mm × 74 mm fin cores. The major fin geometries are listed as follows: fin height h, fin wavelength s, fin thickness t, fin width b, fin angle α and staggered fin wavelength s_0.

Fins pressed by one cold stamping mould pair could only be regulated in fin height h and fin wavelength s in a particular range, so every fin scheme varying in the other parameters is correspondent to different mould pairs. Therefore, a lot of mould pairs are needed in order to study all fin geometrical parameters inducing fin shape deviations. What is more important but generally ignored, mould wear is serious during

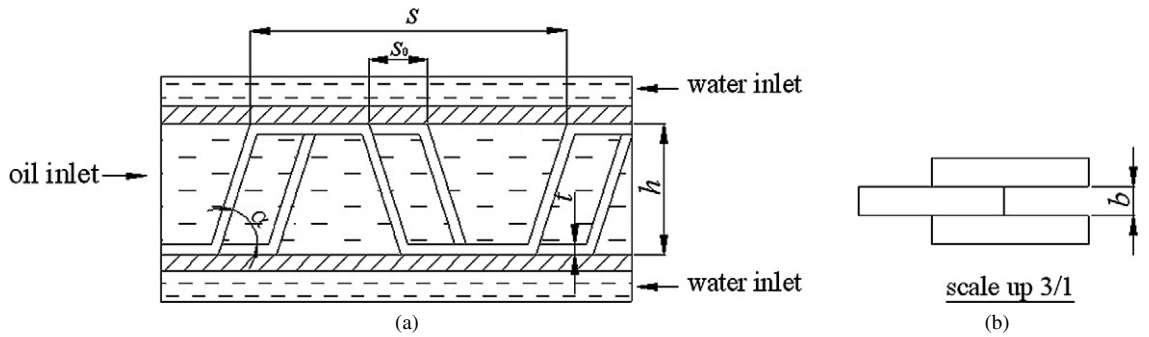

Fig. 2. HPD type fin geometrical parameters. (a) Cross section; (b) Fin top.

Table 1
Fin schemes

Variable	h (mm)	s (mm)	b (mm)	α (deg)	t mm	s_0 (mm)	Experiment	Simulation
Baseline	3.2	7.9	1.5	80	0.3	$s/4$	Y	Y
Fin height	3.0 3.4 3.6	7.9	1.5	80	0.3	$s/4$	Y	Y
Fin wavelength	3.2	6.81 8.45 4.67 14	1.5	80	0.3	$s/4$	Y N	Y Y
Fin width	3.2	7.9	1.0 2.0 3.0	80	0.3	$s/4$	N	Y
Fin angle	3.2	7.9	1.5	70 85 90	0.3	$s/4$	N	Y
Fin thickness	3.2	7.9	1.5	80	0.1 0.2 0.5	$s/4$	N	Y
Staggered fin wavelength	3.2	7.9	1.5	80	0.3	$s/7$ $s/6$ $s/5$	N	Y

pressing steel fins, thus fins pressed by the same mould pair in different periods will obviously exhibit performance deviation. Consequently, aiming at getting rid of above errors, six fin schemes were continuously manufactured for geometrical influence test only varying in fin height and fin wavelength by the same pressing mould pair with about 500 thousand pressing times, in which mould wear would be proved stable latter. As for compensation, numerical models with the same geometries were built and compared, and the other four parameters are numerically investigated by another fourteen models. In engineering applicable range, the experimental and numerical HPD type fin schemes are chosen in Table 1, where fin wavelength s is set that it could divide fin core length exactly.

3. Mathematical analysis

3.1. Governing equations

Both oil and water are considered constant-properties because of low temperature difference. The flows are steady, three-dimensional and incompressible. Lubricant oil floating through fins is characterized by small hydraulic diameter and low Reynolds number under practical work conditions, hence is laminar inside. Radiant heat transfer and viscous energy dissipation are neglected. The dimensionless equations for continuity, momentum and energy are expressed as [27,28]:

$$\frac{\partial u_i}{\partial x_i} = 0 \tag{1}$$

$$\frac{\partial}{\partial x_j}(u_i u_j) = -\frac{\partial p}{\partial x_i} + \frac{1}{Re}\left(\nabla^2 u_i\right) \tag{2}$$

$$\frac{\partial}{\partial x_j}(\Theta u_j) = \frac{1}{Re_{\mathrm{dh}} Pr}\left(\nabla^2 \Theta\right) \tag{3}$$

where, $Re_{\mathrm{dh}} = \rho u d_{\mathrm{h}}/\mu$, $d_{\mathrm{h}} = 4V_{\mathrm{free}}/A_{\mathrm{wet}}$. Nondimensionalized parameters are used in above equations: velocity is nondimensionalized with uniform oil inlet velocity, length with oil side hydraulic diameter, and pressure with ρu^2. The dimensionless temperature Θ is defined as follows:

$$\Theta = \frac{T_{\mathrm{w}} - T}{T_{\mathrm{w}} - T_{\mathrm{in}}} \tag{4}$$

Water side is described by the standard k–ε model [29], the constants in which are $C_\mu = 0.09$, $C_{1\varepsilon} = 1.44$, $C_{2\varepsilon} = 1.92$, $\sigma_{\mathrm{k}} = 1.0$ and $\sigma_\varepsilon = 1.3$. Wall function is employed near plate walls to decrease inaccuracy in that region [30].

3.2. Modeling, numerical procedure and boundary conditions

All models are similar in structures, thus a program was designed with ANSYS Parametric Design Language (APDL) for batch construction of hexahedral structural grid models which were refined near walls. The grid models were sent to Fluent for calculation. The whole fin array size was limited as 56 mm × 12 mm to control computational scale. The governing equations were solved by SIMPLE algorithm [29]. Hybrid system was employed for the treatment of convection and diffusion terms. To ensure simulation accuracy, grid independency had been checked by changing node population. Taken the baseline as an example, three grid schemes, $397 \times 80 \times 52$, $298 \times 60 \times 39$ and $238 \times 48 \times 31$ were tested. It was concluded that the relative errors of both the average Nusselt number and friction factor are less than 3% for the two former schemes at $Re = 300$. Therefore, the $298 \times 60 \times 39$ grid scheme (Fig. 3) is adopted considering a balance between calculation speed and precision.

In Fig. 3, the inlet temperatures for oil and water are respectively 115 °C and 93 °C. Mass flow rate inlet as boundary condition was given at oil side and velocity inlet at water side.

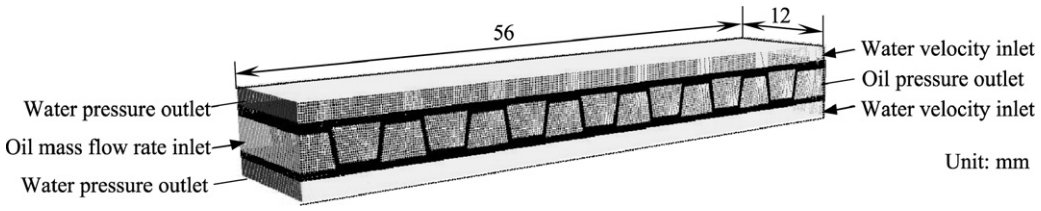

Fig. 3. Model and grid size.

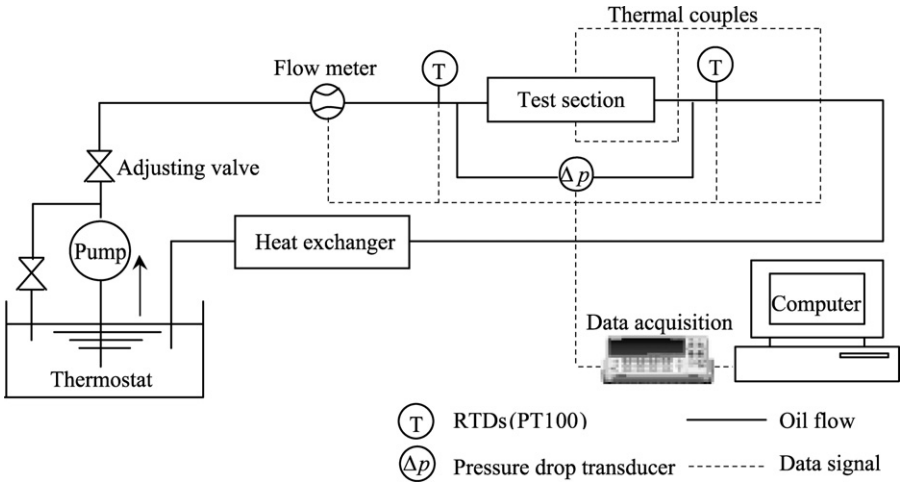

Fig. 4. Test rig system.

The outlet pressures for both liquids were adopted 0 Pa respectively, and symmetry boundary conditions were applied to the other four lateral faces for whole computational zone. Water velocity was kept constant and oil mass flow points for each scheme were evenly selected between 200 $\mathrm{kg\,h^{-1}}$ and 1000 $\mathrm{kg\,h^{-1}}$ for simulation.

4. Experimental analysis

Conventionally, the test specimens are water-cooled and multi-channel heat exchangers. Convective heat transfer coefficients are average values of whole assembly, of which uneven fluid distributions for each channel will bring in errors. Therefore, in this study an electrically heated single fin core was adopted as test object for each experiment.

The test rig was composed of a test section, an oil loop and a data transducing/acquisition system, as shown in Fig. 4. CD 15W/40 lubricant oil was used as work fluid. A thermostatic oil bath was installed to control oil inlet temperature of the test section. A Coriolis mass flow meter was set to measure oil mass flow rate. A plate heat exchanger was installed in oil return loop to cool down the heated oil. Two pre-calibrated resistance temperature detectors (RTDs) were fixed at the inlet and outlet of the test section to measure oil temperature, and a pressure difference transducer was adopted to acquire oil pressure drop through fin cores. Signals were collected by a Keithley 2700 6(1/2)-digit multimeter/data acquisition system.

Details of the test section are revealed in Fig. 5 with a sandwich construction. A fin core was fixed between two pre-

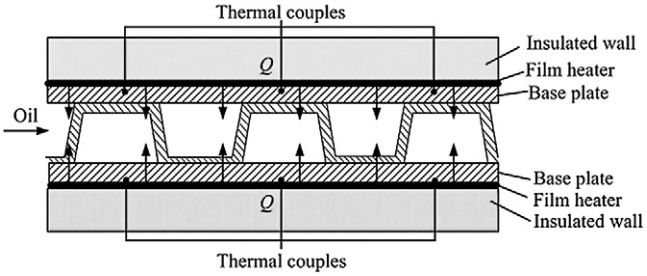

Fig. 5. Test section details.

cisely grinded copper plates as base plates to ensure good contact. Fifteen Φ2 mm holes were drilled on each base plate for copper-constantan thermocouple installation to measure wall temperature. A film heater was firmly adhered to the back of each base plate, the power of which was adjusted by a high precision voltage regulator. High conductivity paste was filled to each contact pair to minimize contact heat resistance. A piece of 20 mm thick plexiglass plate covered each heater as insulation layer. All components were firmly clamped together as close as possible. The whole test section was wrapped by glass wool batt and placed in a thermostatic box.

For each scheme, inlet temperatures of both fluids were set the same as those of simulation. Five oil mass flow rate points were evenly selected between 200 $\mathrm{kg\,h^{-1}}$ and 1000 $\mathrm{kg\,h^{-1}}$. It took at least 90 minutes to reach a steady state at each measuring point. Data are collected when all signals were invariable and the heat balance deviation was within 3%. The collection

repeated three times for each test point at certain intervals to validate result reproducibility.

5. Results manipulation

5.1. Colburn factor and friction factor deduction

Colburn factor and friction factor are adopted for fin performance evaluation. As the flow approaches a periodic fully developed regime, the average heat transfer coefficient approaches a constant value. From measured data, the obtained heat transfer coefficient, h_{oil}, is the average value over the whole tested fin array. According to analyzing the whole heat exchange system, the following equation is gotten:

$$m_{\mathrm{oil}}c_{\mathrm{oil}}(T_{\mathrm{out}}-T_{\mathrm{in}})=\frac{\Delta T_{\mathrm{m}}}{\frac{1}{h_{\mathrm{oil}}\cdot\eta_{\mathrm{o}}\cdot A_{\mathrm{oil}}}+\frac{2t_{\mathrm{cu}}}{\lambda_{\mathrm{cu}}\cdot A_{\mathrm{cu}}}} \tag{5}$$

where, η_{o} means heat transfer surface efficiency [3],

$$\eta_{\mathrm{o}}=1-\frac{A_{\mathrm{f}}}{A_{\mathrm{oil}}}\left(1-\frac{\tanh(l\cdot\sqrt{2h_{\mathrm{oil}}/\lambda_{\mathrm{f}}t_{\mathrm{f}}})}{l\cdot\sqrt{2h_{\mathrm{oil}}/\lambda_{\mathrm{f}}t_{\mathrm{f}}}}\right) \tag{6}$$

here, $l=h/2-t$. h_{oil} and η_{o} are interdependent by substituting Eq. (6) to Eq. (5), so iteration method should be adopted to calculate h_{oil}. Accordingly, Nusselt number could be worked out as follows:

$$Nu_{\mathrm{dh}}=\frac{h_{\mathrm{oil}}d_{\mathrm{h}}}{\lambda_{\mathrm{oil}}} \tag{7}$$

Then Colburn factor j is derived as [10]:

$$j=\frac{Nu_{\mathrm{dh}}}{Pr^{1/3}\cdot Re_{\mathrm{dh}}} \tag{8}$$

while, friction factor f is defined as [10]:

$$f=\frac{d_{\mathrm{h}}}{4L}\cdot\frac{\Delta p}{(1/2\rho_{\mathrm{m}}u^2)} \tag{9}$$

Oil pressure losses at the positions of inlet, outlet, joint and hose are included in the total pressure difference and bring errors to the calculation. In order to eliminate this deviation, other tests for bare channels without fins are done corresponding to different channel heights; then Δp is obtained by removing above excessive pressure drop in the latter from total pressure difference in the former.

5.2. Surface thermal-hydraulic performance judgment

It is a focus for manufacturers to select the optimum surfaces with larger Nusselt number, Colburn factor and smaller friction factor. Therefore, a practical criterion judging global thermal-hydraulic performance is put forward by Saha [31], a general dimensionless parameter promoted as follows:

$$JF=\frac{j/j_{\mathrm{ba}}}{(f/f_{\mathrm{ba}})^{1/3}} \tag{10}$$

where, the subscript 'ba' means bare channel. JF is a 'the larger the better' parameter; namely, the enhanced surfaces with larger JF factor have better global thermal-hydraulic characteristics.

6. Parametrical study

According to the aforementioned fin schemes, influences of geometrical parameters as fin height and fin wavelength are experimented and compared with simulated results. The data determined from the only available models on the HPD type fins by Muzychka [3] are compared with those of corresponding test and simulation.

Fig. 6 shows the tested, simulated and Muzychka's j factors, f factors and JF factors of schemes in fin height from 3.0 mm ~ 3.6 mm under different oil Reynolds numbers. For three cases the results have similar distributions: both j factor and f factor grow with fin height increasing at the same Reynolds number. With the growth of fin height, oil side heat transfer area increases while fin efficiency decreases, and the results imply that the former influence exceeds that of the latter. For friction factor f, the following equation is deduced from Eq. (9),

$$f=\frac{\mu Re}{2L\rho_{\mathrm{m}}^2}\cdot\frac{\Delta p}{u^3} \tag{11}$$

Apparently, f factor is decided by the ratio of Δp to u^3 at the identical Reynolds number. Both u and Δp drop with fin height growing, and the increase of f factor indicates that u^3 item drops more seriously than Δp. JF factor also grows with the increase of fin height in the studied range.

The experimented and calculated influences of fin wavelength are shown in Fig. 7 for the present test, simulated and Muzychka's data. The simulated results show that j factor increases when fin wavelength grows in the studied range, while both the tested and Muzychka's j factor curves almost overlap. Simultaneously, Δp declines more quickly than u^3, resulting in the reduction of f factor for the three cases along with fin wavelength increasing. JF factor declines with fin wavelength decreasing in the tested range.

From above phenomena, although both tendencies of the present experimental data and simulated data agree well, their values vary evidently. The tested j factor is smaller than that of the simulated data, while the tested f factor exceeds the corre-

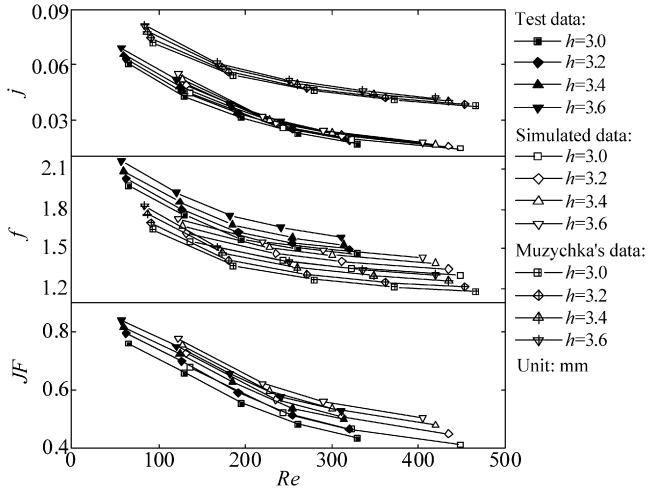

Fig. 6. Influence of fin height in fin performance.

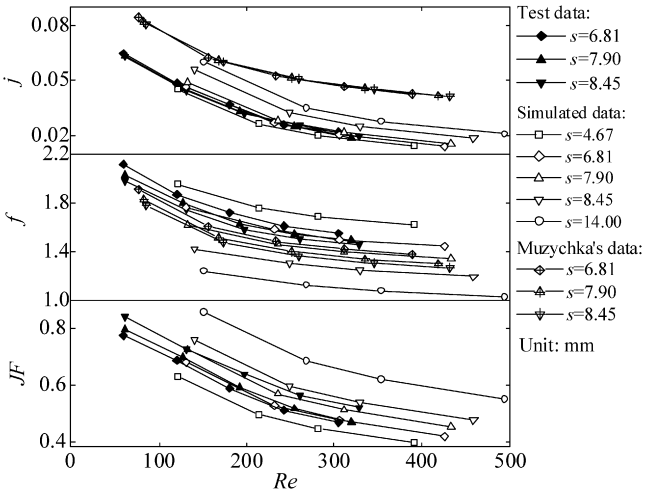

Fig. 7. Influence of fin wavelength in fin performance.

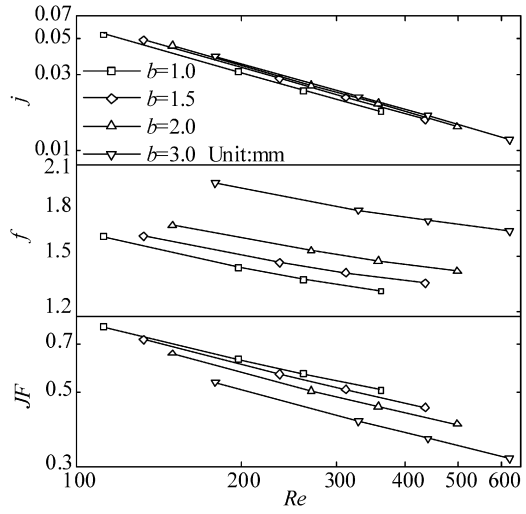

Fig. 8. Influence of fin width in fin performance.

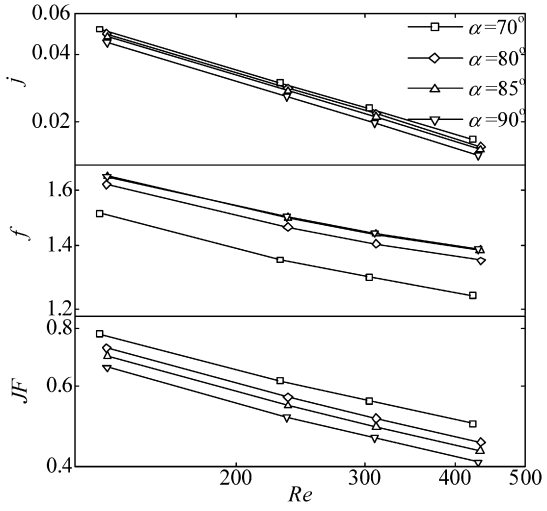

Fig. 9. Influence of fin angle in fin performance.

sponding simulated result especially in Fig. 7. The reasons are considered as follows:

(1) Burrs at separating surfaces [11,14]. The increases of mould wear and die clearance result in significant variations in the burrs on fin edges. The burrs increase the form drag thus raises the overall friction factor, which was also mentioned by Kays and London [10]. In addition, the burrs help to enhance heat transfer by increasing surface areas; however, above experiments show that this effect is not prominent.
(2) Fin shape uncertainty [14,15]. Due to manufacturing tolerances of stamping mould pairs and fin material rebound effects after pressing, distinct geometrical discrepancies exist between actual and simulated fins. The geometrical uncertainty mainly focuses on fin angle, staggered fin wavelength and chamfer. However, this integrated geometrical error is somewhat complicated and uncertain, consequently induces the uncertain influence in fin performance.
(3) Experiment uncertainty. This uncertainty includes the physical properties of coolants and the measurements of temperature, pressure and flow rate. By using the estimation method [33], the relative error is 4.89%∼5.5% for convective heat transfer coefficient and 1.39%∼8.8% for friction factor.

Above three integrated reasons induce the deviations between the present tested and simulated results. Moreover, in Figs. 6 and 7, j factor and f factor determined from Muzychka's model in corresponding to the same Reynolds number are compared to the present simulated and experimental data. Both figures show Muzychka's data for j factors are larger than those of simulated and experimental data, while Muzychka's f factors are lower than those of simulated and experimental data. The reason mainly lies in fin material difference. The steel used in present study is much harder compared to aluminum and brass adopting by Muzychka, thus mould wear is much more serious, resulting in producing more burrs. In addition, fin shapes by these materials are slightly different.

According to above comparisons on two geometrical parameters, fin global performance is always overestimated by numerical analysis. However, considering that the tendencies between the tested and simulated results show good agreement, it is taken as granted that in this paper it is instructive to adopt the simulation for evaluating and comparing fin performance. Thereinafter the other four geometrical parameters are investigated by simulation.

Fig. 8 displays the simulated relationship between fin width and fin performance. Both j factor and f factor increase since convective heat transfer coefficient and pressure drop ascend as fins are widened. However, JF factor has an opposite changing tendency.

Corresponding studies on fin angles are hardly seen in available literatures; however, this parameter has evident effect on fin performance, which is shown in Fig. 9. With fin angle growing, j factor descends but f factor increases. The intervals among f factor curves shrink with the growth of fin angles, and the curves at 85° and 90° fin angles almost overlap, implying that the effect on flow resistance is not prominent around 85°.

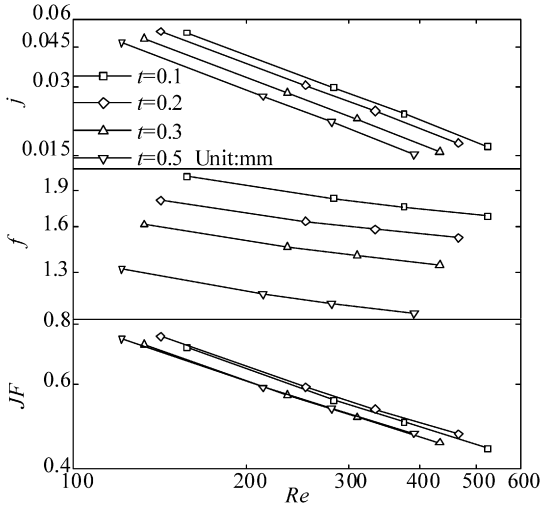

Fig. 10. Influence of fin thickness in fin performance.

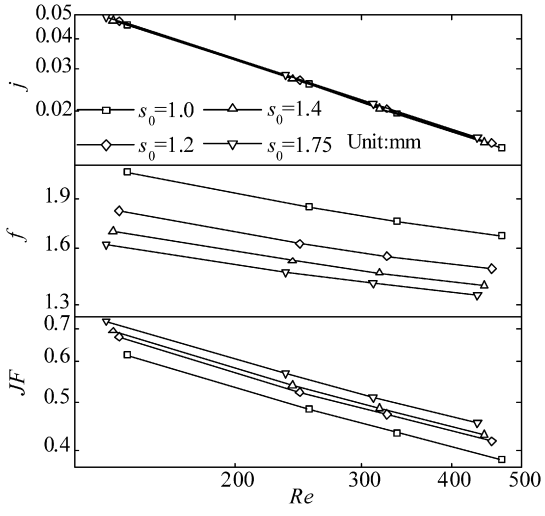

Fig. 11. Influence of staggered fin wavelength in fin performance.

According to the comparison of *JF* factor curves, fins with smaller fin angles have better global performance.

Fig. 10 reveals the effect of fin thickness on fin performance. As fin stock is thickened, flow channel is shrunk and flow velocity is accelerated, which are quite contrary to those caused by fin height growth. Thus their tendencies are just opposite; scilicet both j factor and f factor decline with fin thickness increasing. Fig. 10 shows that fin global performance first rises from 0.1 mm to 0.2 mm in thickness then drops from 0.2 mm to 0.3 mm. Fins with the thicknesses of 0.3 mm and 0.5 mm almost have the same *JF* factors.

Staggered fin wavelength is commonly set as a quarter of fin wavelength in practice. Fig. 11 demonstrates its rationality. All j factor curves overlap, indicating that it contributes little to fin heat transfer performance. Nevertheless, shorter staggered wavelength corresponds with much higher f factor at identical Reynolds number below $s/4$. Since the fins at $s_0 > s/4$ are exactly the same as those at $s_0 < s/4$, above regulation reverses when staggered fin wavelength exceeds $s/4$. Therefore, f factor finds their minimum values while $s_0 = s/4$. Fig. 11 tells that fins show prime global performance when $s_0 = s/4$.

Table 2
Control factors and levels

Levels	h (mm)	s (mm)	b (mm)	t (mm)	α (deg)	s_0 (mm)
1	2.8	4.67	1.0	0.1	70	$s/4$
2	3.0	6.81	1.5	0.2	75	$s/5$
3	3.2	7.90	2.0	0.3	80	$s/6$
4	3.4	8.45	2.5	0.4	85	$s/7$
5	3.6	14.00	3.0	0.5	90	$s/8$

Generally speaking, each geometrical parameter has its unique influence in thermal-hydraulic characteristics with unequal importance. In order to optimize fin shapes, the importance of above parameters is required to be analyzed and compared.

7. Importance analysis and shape optimization

Taguchi method is utilized to find geometrical parameter importance. Usually Orthogonal Array (OA) is adopted for scheme designs, of which the schemes are still excessive if many levels and factors exist. This paper adopts uniform design method [32] to replace OA method for further reducing scheme numbers while keeping enough precision and good deconcentration. According to Taguchi method design principles, in order to select the levels of control factors more efficiently, the calculated *JF* factor of each scheme is transferred into the ratio of signal to noise (*SN*) [20]:

$$SN = 10\log\left(\frac{1}{Z} \times \frac{(S_\mathrm{m} - V_\mathrm{e})}{V_\mathrm{e}}\right) \tag{12}$$

where, $Z = \sum_{i=1}^{m} u_i^2$, $S_\mathrm{m} = (\sum_{i=1}^{m}(u_i \times JF_i))^2/Z$, $V_\mathrm{e} = (\sum_{i=1}^{m} JF_i^2 - S_\mathrm{m})/(m-1)$, u_i is the ith oil velocity. JF_i is the ith *JF* factor. Larger *SN* ratio is preferred for optimization. The degree of influence for each parameter in fin performance is evaluated by contribution ratio (*CR*),

$$CR_j = \frac{SN_{\max,j} - SN_{\min,j}}{\sum_{j=1}^{m}(SN_{\max,j} - SN_{\min,j})} \tag{13}$$

where, $SN_{\max,j}$ and $SN_{\min,j}$ denote the maximum *SN* and minimum *SN* respectively for the jth control factor. Similarly to *SN*, *CR* is also a 'the larger the better' dimensionless parameter.

7.1. Uniform design schemes and solutions

In the past 20 years, uniform designs have been widely used in computer and industrial experiments when the underlying model is unknown [32]. To establish a uniform design one needs to find suitable design points which are recommended to be uniformly scattered on experimental domain. For the present study, six geometrical parameters as h, s, b, t, α and s_0 are promoted as control factors, and each parameter has five levels based on engineering practice as listed in Table 2. For the sake of corresponding to the experimentally available fin wavelength, five nonuniformly scattered fin wavelength levels are selected to facilitate comparison, while the other five geometrical

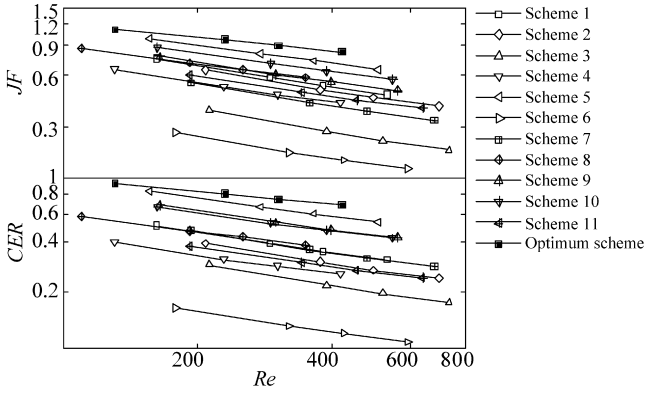

Fig. 12. *JF* and *CER* comparison for each scheme.

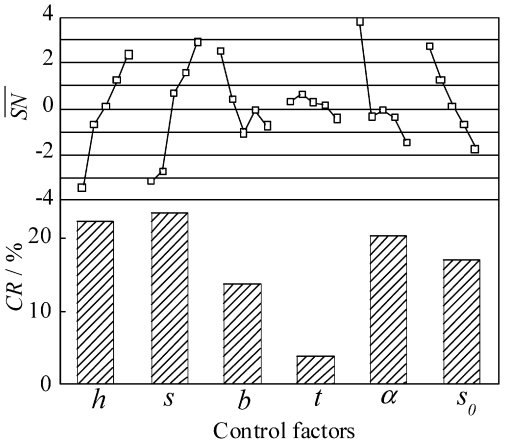

Fig. 13. Contribution comparison for each scheme.

Table 3
Uniform design schemes

Scheme No.	h (mm)	s (mm)	b (mm)	t (mm)	α (deg)	s_0 (mm)	SN
1	2.8	4.67	1.5	0.3	85	$s/8$	−2.8049
2	2.8	6.81	2.0	0.5	75	$s/8$	−4.0757
3	3.0	7.90	3.0	0.2	90	$s/7$	−2.5229
4	3.0	8.45	1.0	0.5	80	$s/7$	1.1592
5	3.2	14.00	1.5	0.2	70	$s/6$	3.7287
6	3.2	4.67	2.5	0.4	90	$s/6$	−3.5230
7	3.4	6.81	3.0	0.1	80	$s/5$	−1.3342
8	3.4	7.90	1.0	0.4	70	$s/5$	3.8841
9	3.6	8.45	2.0	0.1	85	$s/4$	1.9992
10	3.6	14.00	2.5	0.3	75	$s/4$	3.3750
11	3.6	14.00	3.0	0.5	90	$s/8$	1.6792

parameters have evenly distributed levels. As for OA method, the orthogonal table $L_{25}(5^6)$ is needed having 25 schemes. In contrast, uniform table $U_{11}(11^6)$ has only 11 schemes, in which scheme number is greatly reduced while levels are still fully decentralized. Simulations were conducted then *JF* and *SN* were calculated in Table 3.

Fig. 12 shows *JF* factor of each scheme. It is seen that the 5th scheme has the best global thermal-hydraulic performance while the 6th scheme has the worst performance among these eleven schemes.

7.2. Parameter importance analysis and geometries optimization

SN is arithmetically averaged to get the mean *SN* ($\overline{SN}$) at each level for every control factor. Then *CR* of each factor is calculated. Fig. 13 reveals their contribution comparisons, which demonstrate that s, h and α are the three primary factors for fin global performance. s_0 is also important; however, it generally adopts $s/4$ which is already the optimum value. The *CR* values of both fin width and fin thickness are small, thus their influences could be neglected in pre-design procedure. Consequently, attention is suggested to be focused on s, h and α for fin performance promotion.

According to $\overline{SN}$ comparisons in Fig. 13, the optimum geometrical parameters for available fin levels mentioned above are obtained as follows: $h = 3.6$ mm, $s = 14$ mm, $t = 0.2$ mm, $b = 1.0$ mm, $\alpha = 70°$ and $s_0 = s/4$. The optimum fin model is analyzed and compared in Fig. 12, showing that its global performance is 16% larger than that of the 5th scheme at $Re = 430$. This proves the effectiveness of Taguchi method combined with uniform design for fin shape optimization.

7.3. Cost-based fin performance verification

Fin cost is not taken into account in above optimization, which is highly sensitive to manufacturers. In order to give a more practical standard for fin effectiveness judgment, the 'Cost-Effect Ratio' (*CER*) is proposed to evaluate fin global performance,

$$CER = \frac{JF}{C} \tag{14}$$

where C is defined as the average cost ratio of whole plate-fin to two base plates per unit plate area. Since the costs of plates and fins are mainly decided by raw material prices, then

$$C = \frac{M_\mathrm{f} \cdot P_\mathrm{f} + M_\mathrm{p} \cdot P_\mathrm{p}}{M_\mathrm{p} \cdot P_\mathrm{p}} \tag{15}$$

where P_f and P_p are the unit prices of fin and plate raw materials. M_f and M_p are the material mass of fins and plates respectively. Define $\beta = M_\mathrm{f}/M_\mathrm{p}$, Eq. (14) is written as

$$CER = \frac{JF}{1 + \beta \cdot P_\mathrm{f}/P_\mathrm{p}} \tag{16}$$

Obviously, fins with larger *CER* have better global performance with less raw material cost.

Assuming that material density and the unit price of plates and fins are exactly the same for simplification, adopting plate thickness as 0.6 mm, *CER* comparison of above 12 schemes including the previous optimum model is also displayed in Fig. 12. It is seen that considering material consumption, the relative positions of these curves slightly vary compared with those of $\overline{SN}$. *CER* of the optimum model is 12%∼27% larger than that of the 5th scheme in the calculated Reynolds number range, verifying that the previous optimum scheme is also economical based on above simplifications.

8. Influence analysis of pressing mould wear in steel fin performance

As mentioned before, pressing mould wear is important to steel fin global performance. Since low carbon cold rolled steel is relatively harder than other fin materials such as aluminum and brass, mould wear is much more serious. Burrs appear on fin surfaces, which increase fin pressure loss and deteriorate cleanliness. However, little researches on this influence have been found in available literatures. This paper also attempts to preliminarily investigate mould wear influence in fin performance.

8.1. Experiments on pressing mould wear influence in fin performance

The fin pressing mould pair was made of Cr12MoV alloy tool steel. The mould pair underwent vacuum heat treatment including twice preheating, 1020 °C∼1040 °C quenching with 20 °C∼60 °C vacuum quenching oil and 240 °C vacuum tempering. Fins pressed by a mould pair in production lines were inspected for wear conditions which were not included in aforementioned fin schemes. Sampling frequencies were much denser at the beginning and afterwards twice a day averagely. The mould pair pressed 1400 thousand times before next overhauling. During this period, eleven fin samples were taken out from production line for wear test.

Fig. 14(a) shows friction factor distributions of fins varying in pressing times at different Reynolds numbers. It is clearly seen that f factor varies along with pressing times at identical Reynolds number. Fig.14(b) displays f factor first rises distinctly from the beginning to about 100 thousand pressing times, and then slowly drops back to a lower degree before 510 thousand pressing times. During 510 to 1050 thousand times, the curve slowly climbs up again, and the values of f factor almost reach those of 100 thousand pressing times by the end of this period. During 1050 to 1400 thousand pressing times, f factor continues to increase and fin quantity prominently degrades. The cut edges of mould pair need to be manually ground frequently to keep blade sharpness. After 1400 thousand times, it is unable to keep fin qualities only by grinding mould blade and another overhauling is needed. The maximum deviation of f factor reaches 7.3% for fins pressed in different periods. Based on above analysis, the whole mould wear process is divided into three stages: initial wear from 0 to 100 thousand times, stable wear from 100 to 1050 thousand times, and overdrive wear after 1050 thousand pressing times.

J factors are also determined experimentally as revealed in Fig. 14(c). The variational tendencies of j factors are exactly reverse to those of f factor: j factors decrease distinctly from the beginning to 100 thousand pressing times, and they slightly fluctuate and tend to be stable in the second stage from 100 to 1050 thousand times. After 1050 thousand times, j factors again exhibit declining tendencies, which is attributed to the local variation of fin shapes induced by die clearance increasing along with mould wear aggravation.

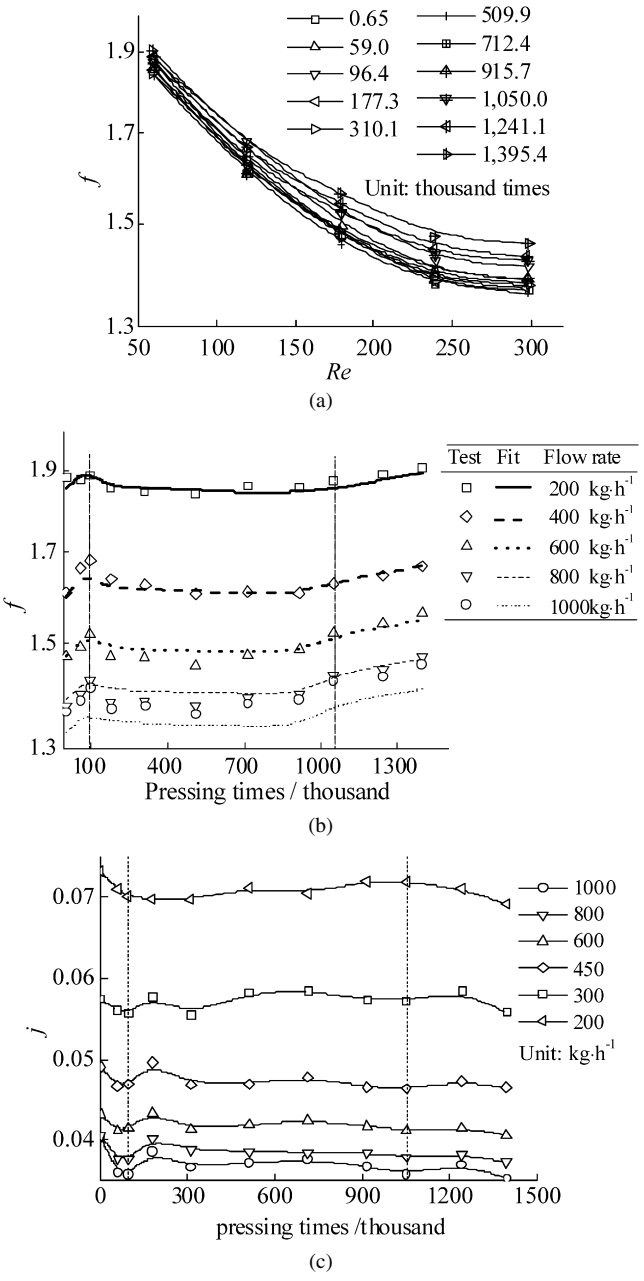

Fig. 14. f factor and j factor varying in pressing times at different Reynolds number. (a) f factor vs. Re; (b) f factor vs. pressing times; (c) j factor vs. pressing times.

8.2. Regulations and principles for pressing mould wear influence in fin performance

According to the experiments, it is considered that f factor for this manufactured fin scheme is mainly affected by pressing times and Reynolds number, and then the following equations are derived:

$$f = \begin{cases} 4.0674n^{0.004417}Re^{-0.1992} \\ \quad 0 < n \leqslant 1.0 \times 10^5 \\ 4.2885n^{-0.004107}Re^{-0.1921} \\ \quad 1.0 \times 10^5 < n < 1.05 \times 10^6 \\ 1.3345n^{0.07583}Re^{-0.1765} \\ \quad n \geqslant 1.05 \times 10^6 \end{cases} \tag{17}$$

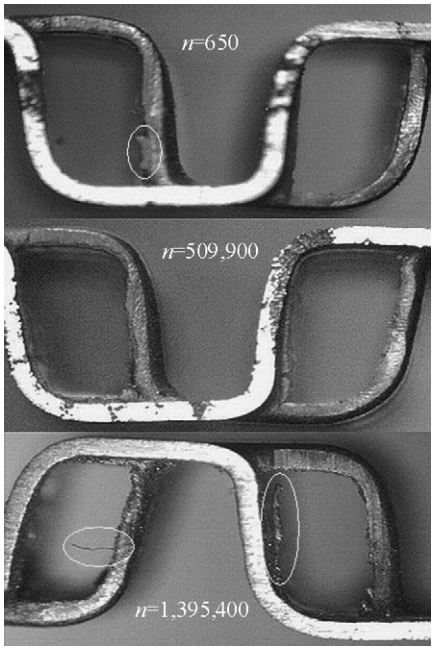

Fig. 15. Separating surface qualities with different pressing times.

The relative errors between Eq. (17) and experimental data are −2.329%∼2.695%, −3.056%∼4.832% and −1.702%∼2.194% respectively.

As for j factors, their curves always fluctuate along with pressing times, which brings difficulties in quantitative description.

Fig. 15 reveals the cross section of fins pressed by the same mould pair in different mould pressing times. Burrs are found on separating surfaces, some of which are encircled in the figure. For fins produced by mould pair with 650 pressing times, the separating surfaces are relatively smooth. A few large burrs exist on tooth roots while small burrs are scarce. For fins produced after 509.9 thousand pressing times, small burrs appear at fin edges instead of large burrs. For fins produced by mould pair with 1395.4 thousand times, burrs of all scales are found adhering to fin edges, and fin surfaces are relatively rough. Since these burrs are directly related to mould wear, it is concluded that the mould pair is in running-in period before 100 thousand pressing times, and then their wear conditions are stable until 1050 thousand pressing times. The blades are blunt after 1050 thousand times resulting in the serious increase of die clearances and the degradation of product qualities. Obviously, fins produced in stable mould wear stage have less large-scale burrs, which bring another benefit of keeping oil cleanly besides stable performance. Thus this stage is preferred for high-quality fin manufacturing.

The lifetime for this type of mould pair is suggested not to exceed 1050 thousand pressing times, otherwise product qualities would quickly deteriorate.

9. Conclusions

Aided by a single fin core test rig and CFD software, experimental and numerical studies were conducted for 20 schemes of the HPD type steel offset strip fins. According to comparisons, the effects of each geometrical factor on fin thermal-hydraulic performance were derived. Results show that within the studied range, j factor rises with the enlargements of h, s and b, while f factor decreases with the increases of s, t and s_0. By applying Taguchi method and uniform design, the importance of each geometrical factor on fin performance was studied, verifying that s and h have the most significant contributions. Fin geometries were optimized for best global performance and the 'cost-effect ratio' was proposed and compared. Mould wear influence in fin performance was preliminarily tested. Influence regulations and principles were deduced, and the performance variation is attributed to burrs produced by fin manufacturing. This research is expected to extend the understanding of steel HPD type offset strip fin performance, which would be helpful for steel fin design, matching and pressing mould improvement.

Since the optimized fins are proposed by simulation, necessary experiments on this fin shape are still needed for verification. Moreover, this research on mould wear influence is just a beginning; the proposed equations are only applicable for this type of mould pair and steel fins studied in this paper, thus lots of works are further required for detailed researches.

Acknowledgements

The research was supported by Zhejiang Yinlun machinery Co., Ltd. The authors acknowledge the support from Mr. W.F. Zhang. This paper would not have been accomplished without his help.

References

[1] S.W. Chang, Forced heat convection in a reciprocating duct fitted with 45 degree crossed ribs, International Journal of Thermal Sciences 41 (2002) 229–240.
[2] K. Yakut, B. Sahin, Flow-induced vibration analysis of conical rings used for heat transfer enhancement in heat exchangers, Applied Energy 78 (2004) 273–288.
[3] Y.S. Muzychka, Analytical and experimental study of fluid friction and heat transfer in low Reynolds number flow heat exchangers, PhD thesis, University of Waterloo, Waterloo, Canada, 1999.
[4] W.M. Kays, A.L. London, Heat transfer and flow friction characteristics of some compact heat-exchanger surfaces, Part I. Test system and procedure, Journal of Heat Transfer 72 (1950) 1075–1085.
[5] W.M. Kays, The basic heat transfer and flow friction characteristics of six compact high-performance heat transfer surfaces, Journal of Energy Power 1 (1960) 27–34.
[6] D.C. Briggs, A.L. London, The heat transfer and flow friction characteristic of five offset rectangular duct and six plain triangular plate-fin feat transfer surfaces, in: International Developments in Heat Transfer, ASME, New York, 1961, pp. 122–134.
[7] W.M. Kays, A.L. London, Compact Heat Exchangers, McGraw-Hill, New York, 1984.
[8] A. Hachemi, Experimental study of thermal performance of offset rectangular plate fin absorber-plates, Renewable Energy 17 (1999) 371–384.
[9] A.R. Wieting, Empirical correlations for heat transfer and flow friction characteristics of rectangular offset-fin plate-fin heat exchangers, Journal of Heat Transfer 97 (1975) 488–490.
[10] H.M. Joshi, R.L. Webb, Heat transfer and friction in the offset strip fin heat exchanger, International Journal of Heat and Mass Transfer 30 (1987) 69–84.

[11] M.R. Manglik, E.A. Bergles, Heat transfer and pressure drop correlations for rectangular offset strip fin compact heat exchanger, Experimental Thermal and Fluid Science 10 (1995) 171–180.
[12] Y.S. Muzychka, M.M. Yovanovich, Modeling the f and j characteristics of the offset strip fin array, Journal of Enhanced Heat Transfer 8 (2001) 261–277.
[13] Y.S. Muzychka, M.M. Yovanovich, Modeling the f and j characteristics for transverse flow through an offset strip fin at low Reynolds number, Journal of Enhanced Heat Transfer 8 (2001) 243–259.
[14] S. Hu, Heat transfer and pressure drop of liquid cooled offset fin heat exchanger, PhD thesis, University of Maryland, Maryland, USA, 1993.
[15] S. Hu, K.E. Herold, Prandtl number effect on offset fin heat exchanger performance: experimental results, International Journal of Heat Mass Transfer 38 (1995) 1053–1061.
[16] S. Hu, K.E. Herold, Prandtl number effect on offset fin heat exchanger performance: Predictive model for heat transfer and pressure drop, International Journal of Heat Mass Transfer 38 (1995) 1043–1051.
[17] S.V. Patankar, C.H. Liu, E.M. Sparrow, Fully developed flow and heat transfer in ducts having streamwise periodic variations of cross-sectional area, Journal of Heat Transfer 99 (1977) 180–186.
[18] Y.C. Yang, H.L. Lee, E.J. Wei, J.F. Lee, T.S. Wu, Numerical analysis of two-dimensional pin fins with non-constant base heat flux, Energy Conversion and Management 46 (2005) 881–892.
[19] M. Costa, D. Buddhi, A. Oliva, Numerical simulation of a latent heat thermal energy storage system with enhanced heat conduction, Energy Conversion and Management 39 (1998) 319–330.
[20] J.Y. Yun, K.S. Lee, Influence of design parameters on the heat transfer and flow friction characteristics of the heat exchanger with slit fins, International Journal of Heat and Mass Transfer 43 (2000) 2529–2539.
[21] K. Bilen, S. Yapici, C. Celik, A Taguchi approach for investigation of heat transfer from a surface equipped with rectangular blocks, Energy Conversion and Management 42 (2001) 951–961.
[22] K.T. Chiang, Optimization of the design parameters of Parallel—Plain Fin heat sink module cooling phenomenon based on the Taguchi method, International Communications in Heat and Mass Transfer 32 (2005) 1193–1201.
[23] R.N. Kackar, Off-line quality control, parameter design and the Taguchi method, Journal of Quality Technology 17 (1985) 176–188.
[24] G. Taguchi, System of Experiment Design, Quality Resources, International Publications, New York, 1987.
[25] M.S. Phadke, Quality Engineering Using Robust Design, Prentice-Hall, NJ, 1989, p. 334.
[26] C. Ranganayakulu, K.N. Seetharamu, K.V. Sreevatsan, The effects of inlet fluid flow nonuniformity on thermal performance and pressure drops in crossflow plate-fin compact heat exchangers, International Journal of Heat and Mass Transfer 40 (1997) 27–38.
[27] H. Guo, F. Liu, G.J. Smallwood, A numerical study of laminar methane/air triple flames in two-dimensional mixing layers, International Journal of Thermal Sciences 45 (2006) 585–594.
[28] R.S. Matos, T.A. Laursen, J.V.C. Vargas, A. Bejan, Three-dimensional optimization of staggered finned circular and elliptic tubes in forced convection, International Journal of Thermal Sciences 43 (2004) 477–487.
[29] W.Q. Tao, Y.L. He, Z.Y. Li, Z.G. Qu, Some recent advances in finite volume approach and their applications in the study of heat transfer enhancement, International Journal of Thermal Sciences 44 (2005) 623–643.
[30] S.H. Seyedein, M. Hasan, A.S. Mujumdar, Turbelent flow and heat transfer from confined multiple impinging slot jets, Numerical Heat Transfer 27 (1995) 35–51.
[31] A.K. Saha, S. Acharya, Parametric study of unsteady flow and heat transfer in a pin-fin heat exchanger, International Journal of Heat and Mass Transfer 46 (2003) 3815–3830.
[32] K.T. Fang, X. Lu, Y. Tang, J.X. Yin, Constructions of uniform designs by using resolvable packings and coverings, Discrete Mathematics 274 (2004) 25–40.
[33] J.P. Holman, Experimental Methods for Engineers, McGraw-Hill, New York, 1984.